Longitudinal assessment of Alzheimer's beta-amyloid plaquedevelopment in transgenic mice monitored by in vivo magnetic resonance microimaging

Braakman, N.; Matysik, J.; Duinen, S.G. van; Verbeek, F.J.; Schlebs, R.; Groot, H.J.M. de; Alia, A.

Citation
Braakman, N., Matysik, J., Duinen, S. G. van, Verbeek, F. J., Schlebs, R., Groot, H. J. M. de, & Alia, A. (2006). Longitudinal assessment of Alzheimer's beta-amyloid plaquedevelopment in transgenic mice monitored by in vivo magnetic resonance microimaging. *Journal Of Magnetic Resonance Imaging*, *24*(3), 530-536. doi:10.1002/jmri.20675

Version:	Publisher's Version
License:	Licensed under Article 25fa Copyright Act/Law (Amendment Taverne)
Downloaded from:	https://hdl.handle.net/1887/3455642

Note: To cite this publication please use the final published version (if applicable).

Original Research

Longitudinal Assessment of Alzheimer's β-Amyloid Plaque Development in Transgenic Mice Monitored by In Vivo Magnetic Resonance Microimaging

Niels Braakman, MS,[1] Jörg Matysik, PhD,[1] Sjoerd G. van Duinen, MD, PhD,[2] Fons Verbeek, PhD,[3] Reinhard Schliebs, PhD,[4] Huub J.M. de Groot, PhD,[1] and A. Alia, PhD[1]*

Purpose: To assess the development of β-amyloid (Aβ) plaques in the brain with age in the transgenic mouse model of Alzheimer's disease (AD) pathology by in vivo magnetic resonance microimaging (μMRI).

Materials and Methods: Live transgenic mice (Tg2576) and nontransgenic littermates (control) were studied at regular intervals between the ages of 12 and 18 months. Plaques were visualized using a T_2-weighted rapid acquisition with relaxation enhancement (RARE) sequence. Changes in T_2 relaxation times were followed using a multislice multiecho (MSME) sequence. Plaque load and numerical density in MR images were calculated using SCIL image software.

Results: Aβ plaques were clearly detected with the T_2-weighted RARE sequence in the hippocampal and cortical regions of the brain of Tg2576 mice but not in control mice. Following the plaque development in the same animals with age showed that plaque area, number, and size increased markedly, while T_2 relaxation time showed a decreasing trend with age.

Conclusion: These results demonstrate that μMRI is a viable method for following the development of Aβ plaques in vivo, and suggest that this method may be feasible for assessing the effect of therapeutic interventions over time in the same animals.

Key Words: Alzheimer's disease; β-amyloid plaques; MR microimaging; transgenic mouse; longitudinal study
J. Magn. Reson. Imaging 2006;24:530–536.
© 2006 Wiley-Liss, Inc.

ALZHEIMER'S DISEASE (AD) is the most common neurodegenerative disease. It currently afflicts about 10% of the population over 60, and the numbers are rising (1). The neuropathologic features of AD include senile plaques, neurofibrillary tangles, decreased synaptic density, and loss of neurons. The core of senile plaques consists mainly of aggregated amyloidogenic peptide Aβ, which is derived from the β amyloid precursor protein (βAPP). The role of Aβ in AD may be substantial, since soluble Aβ polymers have been reported to be neurotoxic both in vitro and in vivo (2). Although it is not yet clear whether senile plaques themselves are neurotoxic, Aβ plaque formation precedes disease onset by many years and is generally accepted as a biomarker for onset and progression of the disease (3). Early diagnosis of AD is prevented by the difficulty of visualizing Aβ plaques in vivo in the brain. At present, the only definitive diagnosis for AD is postmortem observation of Aβ plaques and neurofibrillary tangles in brain sections (4).

To study the pathogenesis of AD and its development over time, and ultimately to develop adequate therapeutic agents or preventive strategies, it is important to establish noninvasive in vivo imaging methods to visualize Aβ plaques. It is also important to validate whether μMRI is feasible for quantitative monitoring of plaque development with age in the same animals. Imaging methods such as single photon emission computed tomography (SPECT) and positron emission tomography (PET) use ionizing radiation and suffer from low resolution (5). MRI can provide much higher resolution than SPECT or PET without ionizing radiation, and theoretically can resolve individual plaques noninvasively. The first effort to visualize Aβ plaques by MRI in fixed postmortem human brain tissue was made by Benveniste et al (6) using T_2*-weighted MRI at 7T. Subsequently, several different transgenic mouse models of AD pathology

[1]Solid State NMR Group (SSNMR), Leiden Institute of Chemistry, Gorlaeus Laboratoria, Leiden, The Netherlands.
[2]Department of Pathology, Leiden University Medical Center, Leiden, The Netherlands.
[3]Leiden Institute of Advance Computer Science, Leiden, The Netherlands.
[4]Department of Neurochemistry, Paul Flechsig Institute for Brain Research, University of Leipzig, Leipzig, Germany.
*Address reprint request to: A.A., Leiden Institute of Chemistry, Gorlaeus Laboratoria, P.O. Box 9502, 2300 RA Leiden, The Netherlands. E-mail: a.alia@chem.leidenuniv.nl
Contract grant sponsor: Interdisziplinares Zentrum fur Klinische Forschung, Leipzig (IZKF); Contract grant number: TP C18/29; Contract grant sponsors: Cyttron consortium (CYTTRON); The Centre for Medical System Biology (CMSB); Netherlands Organization for Scientific Research (NWO).
Received November 29, 2005; Accepted May 19, 2006.
DOI 10.1002/jmri.20675
Published online 4 August 2006 in Wiley InterScience (www.interscience.wiley.com).

© 2006 Wiley-Liss, Inc.

were used to visualize Aβ plaques either ex vivo in fixed brain (5,7,8) or in vivo using targeted contrast agents (9,10) or amyloidophilic probes (2,11). However, the delivery of these agents requires a relatively invasive procedure. Very recently, initial attempts to detect Aβ plaques in vivo using MRI without the aid of an exogenous plaque-specific contrast agent were performed in transgenic mouse models of AD (12,13) using T_2-weighted spin-echo and T_2*-weighted gradient-echo sequences. Vanhoutte et al (13) used basic T_2*-weighted MRI to visualize plaques associated with iron in vivo in the thalamus region of the brain; however, they failed to detect plaques in the cortex and hippocampus areas, which are the main regions of Aβ deposits in the human brain as well as in transgenic mouse models of AD pathology (14,15). Although imaging of Aβ plaques in vivo without the aid of an exogenous plaque-specific contrast agent still lacks sufficient sensitivity and requires further improvement, to date no longitudinal MR studies to follow the development of Aβ plaques with age in the same animals have been attempted. In recent longitudinal studies concerning the detection of Aβ plaque load in mouse models of AD pathology, postmortem biochemical and/or histological examinations were performed on different mice belonging to different age groups (16).

In the present study, high-field μMRI was used to detect Aβ plaques in a living transgenic mouse model of AD pathology, without contrast agent, and to track the development of plaques with age in the same animals. Our results demonstrate that μMRI is a viable noninvasive method for longitudinal studies to assess Aβ plaque development in quantitative manner, and thus would be invaluable for evaluating new anti-amyloid treatment strategies.

MATERIALS AND METHODS

Transgenic Mice

The transgenic mice used in this study contain as the transgene the Swedish double mutation of the human amyloid precursor protein (APP_{695}), as developed and described previously by Hsiao et al (17). The transgene is expressed in C57B6 breeders. The N2 generation mice of both genders ($N = 5$) were studied at the ages of 12–18 months. Age-matched nontransgenic littermates served as controls. All of the animal experiments were approved by the institutional animal care and animal use committee in accordance with the NIH *Guide for the Care and Use of Laboratory Animals*.

μMRI

All μMRI measurements were conducted on a vertical wide-bore 9.4T Bruker Avance 400WB spectrometer, with a 1000 $mT \cdot m^{-1}$ actively shielded imaging gradient insert (Bruker Biospin GmbH, Germany). The imaging coil used was a 25-mm volume coil, which is best suited to acquire full brain images in both the coronal and horizontal plane because it provides improved SNR homogeneity compared to a surface coil. The system was interfaced to a Linux PC running XWinNMR 3.2 and Paravision 3.02pl1 (Bruker Biospin GmbH, Germany).

For in vivo μMRI measurements the mice were anesthetized using isoflurane (Forene, Abott, UK) inhalation anesthesia, together with air and oxygen (1:1) at 0.3 liter/minute. The anesthetic gas was administered via a special face mask, which also served as a fixation device for the mouse head since it was coupled with a specially designed toothbar to hold the head in place (Bruker Biospin GmbH, Germany). The respiration rate of the mouse inside the probe was constantly monitored by means of a pressure transducer placed on the abdomen. The transducer was connected to a BioTrig acquisition module, which was interfaced to a BioTrig command module and laptop running BioTrig BT1 monitoring software (Bruker Biospin GmbH, Germany).

T_2-weighted MR images were acquired with a rapid acquisition with relaxation enhancement (RARE) sequence (18), which employs a single excitation step followed by the collection of multiple phase-encoded echoes. This reduces the total scan time significantly compared to normal multislice (MS) spin-echo methods. The basic measurement parameters used for the RARE sequence were: echo time (TE) = 10.567 msec (22.45 msec effective), repetition time (TR) = 5–6 seconds, flip angle = 90°, averages = 4, RARE factor (echo train length) = 4, field of view (FOV) = 2.00 × 2.00 cm^2, and image matrix = 256 × 256. This yielded an effective in-plane resolution of approximately 78 μm. Coronal (transverse) image slices (N = 20–30) were acquired from the olfactory bulb to the cerebellum with slice thickness of 0.2 mm spaced 0.2 mm between slices. The horizontal and coronal slices shown in Fig. 1 and those used for longitudinal studies were obtained with slice thickness of 0.5 mm with a total scan time of approximately 25 minutes.

For T_2 mapping, an MS multiecho (MSME) sequence was used. Imaging parameters were: FOV 2.0 × 2.0 cm^2, matrix size 256 × 256, number of averages 2, number of slices 6 with slice thickness of 1 mm, number of echoes = 8 with TE of 8.5, 17.0, 25.5, 34.0, 42.5, 51.0, 59.5, and 68.0 msec, and a repetition time of 1.5 seconds. To calculate the T_2 relaxation time, regions of interest (ROIs) were drawn around the cortex and hippocampus in two adjacent mid-coronal slices. Another ROI in the muscle was used as an internal control according to Helpern et al (7). The means and standard deviation (SD) of the T_2 relaxation times for each ROI were calculated. Mean values were compared using Student's t-test assuming equal variance, and significance was assigned at $P < 0.05$.

Brain Preparation and Histology

Following in vivo MR measurements the mice were deeply anesthetized and transcardially perfused with phosphate-buffered saline (PBS, pH 7.4) followed by 4% buffered paraformaldehyde (Zinc Formal-Fixx, ThermoShandon, UK) through the left cardiac ventricle. After perfusion fixation the brain was dissected out and placed in the same fixative for 48 hours. Following fixation the brain was dehydrated and embedded in paraffin. Subsequently coronal sections (40 μm thick) were carefully cut using a vibratome while maintaining as much as possible the same spatial orientation of mouse

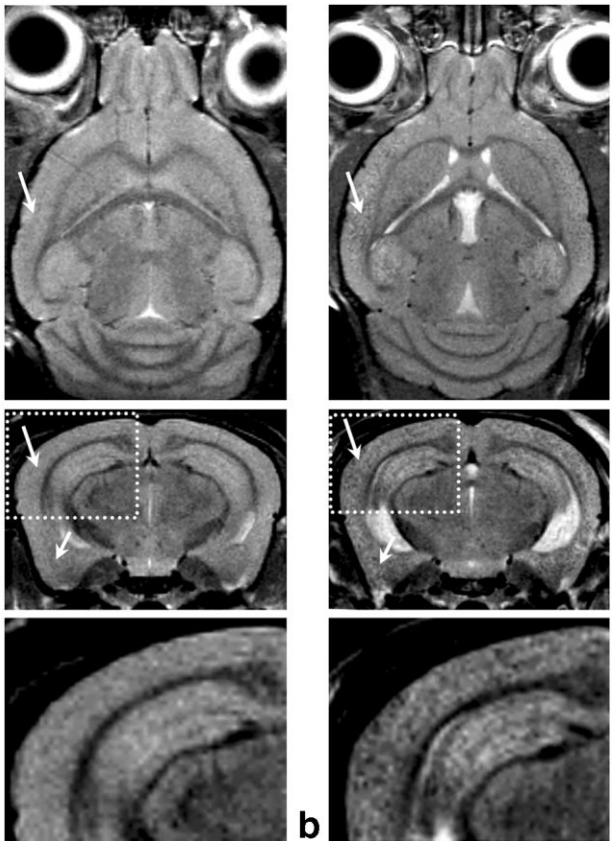

Figure 1. In vivo T_2-weighted MR images of the brain of an 18-month-old control mouse (column **a**) and AD transgenic Tg2576 mouse (column **b**) obtained at 9.4T. Top row: horizontal slices (Bregma: −6 mm); middle row: coronal slices (Bregma: −2.4); bottom row: magnified subsampled insets of the coronal slices showing adequately resolved individual plaques. MR images were obtained with an in-plane resolution of 78 μm × 78 μm (TE = 10.567 msec, TR = 6 seconds, echo train length = 4, averages = 4, total scan time = 25 minutes). Arrows indicate areas with differences in signal intensity between the Tg2576 mouse and its nontransgenic littermate. Numerous circular hypointensities can be clearly observed in the cortical and hippocampal areas of the Tg2576 mouse (column b), while no clear signal hypointensities are visible in the control mouse (column a).

brain as in the MRI experiments. To detect the Aβ plaques, brain sections were subjected to immunohistochemistry using monoclonal anti-amyloid β (6E10) antibody at 1:1000 (Signet Laboratories, Inc). Immunolabeling was visualized by using the ABC kit (Vectastain) according to the manufacturer's instructions.

Detection of redox active iron associated with the Aβ plaques was done histochemically as described previously (19,20). Briefly, the brain sections were incubated for 15 hours in 7% potassium ferrocyanide in aqueous hydrochloric acid (3%) and subsequently incubated in 0.75 mg/mL 3,3′-diaminobenzidine (DAB) and 0.015% H_2O_2 for 5–10 minutes. This method involves the formation of mixed-valence iron (II/III), (Prussian blue) when iron (III) released from iron-containing plaques by the hydrochloric acid reacts with potassium ferrocyanide. The mixed-valance complex then catalyzes the H_2O_2-dependent oxidation of DAB to give a brown color. Images of the histological sections were obtained using a Leica DM RE HC microscope interfaced to a Leica DC500 3CCD digital camera. Quantitative histological analysis of Aβ plaque density and iron-associated plaques was performed by Source Code Interpreter Language (SCIL) image-processing software (21).

For coregistration, immunohistological images were matched with MR slices using common anatomical landmarks, such as the ventricles, corpus callosum, and hippocampal fissure, using PhotoShop 7.0 (Adobe Systems, San Jose, CA, USA). As a result of differences in the slice thickness in μMRI (200 μm) and histology (40 μm), each MR image could be matched with at least four immunostained histological images.

Image Analysis and Quantification

For quantification of Aβ plaque load and numerical density in MR images, image files with calibrated scale markers were imported in the SCIL image-processing environment (21). The brightness of the images was corrected using muscle tissue as the internal control so that the average density measurements in each imported image would be similar. ROIs were manually drawn on the cortex and hippocampus, corresponding to the same anatomical markers used for histological Aβ quantification. Image processing was focused within the ROIs. Dark spots with intensity below a preset threshold value (equal for all MR images) were considered as "Aβ plaques" (10). The number of hypointense plaques within an ROI was established using an object labeling operation, and calibration markers were used to express surface area of each of the ROIs in mm^2. The Aβ plaque load (percentage hypointense area of the ROI) and numerical density of plaques (number of plaques per mm^2) were calculated for the cortex and hippocampus.

RESULTS

Figure 1 shows horizontal (axial) and transverse (coronal) slices through the brain of a living 18-month-old APP transgenic mouse (Tg2576) and its nontransgenic littermate (control) obtained using a T_2-weighted RARE sequence. As can be seen in this figure, numerous dark spots are clearly evident in the cortex and hippocampus areas in both horizontal and transverse MR slices of the Tg2576 transgenic mouse brain (Fig. 1). These hypointense regions could be detected with scan times as short as 25 minutes. Such signal hypointensities were not observed in the brains of control mice (Fig. 1). MR hypointensities can be seen more clearly under higher magnification, as displayed in the bottom row in Fig. 1.

To confirm that the hypointense signals seen in the MR images correspond to Aβ plaques, we compared in vivo MR images of an 18-month-old transgenic mouse with immunostained images obtained from the same mouse brain (Fig. 2). The immunolabeled sections showed that dense-cored plaques are the predominant form of senile plaques in the cortical and hippocampal areas of the Tg2576 transgenic mouse brain (Fig. 2b). Many are giant plaques with core diameters above 100

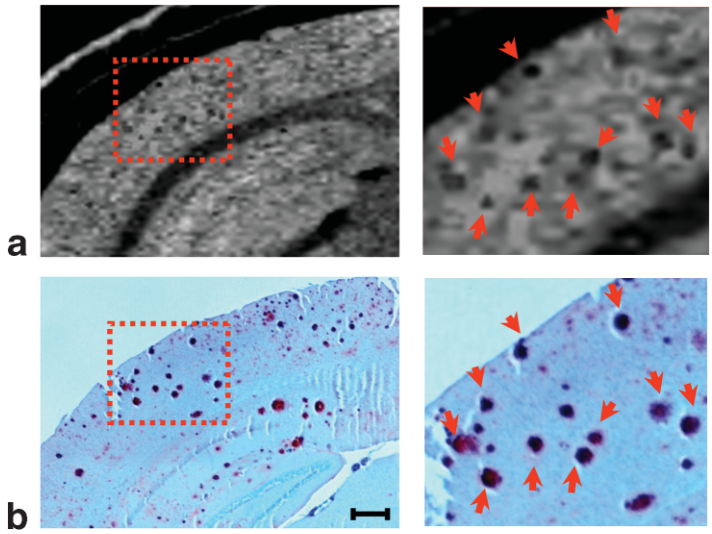

Figure 2. Coregistration of Aβ plaques seen in the brain of an 18-month-old AD mouse by (**a**) in vivo μMRI and (**b**) histological section of the same mouse brain stained with Aβ antibodies. Many MR circular hypointense spots can be matched to immunostained Aβ plaques (arrows), which can be seen more clearly in the higher-magnification insets. Scale bar: 500 μm.

μm. In addition, a few diffuse plaques were also observed. Coregistration of plaques between in vivo μMRI and corresponding immunostained sections illustrates that many circular hypointense regions seen in μMRI correspond to Aβ plaques (Fig. 2). Despite the good correlation between μMRI and immunohistology, however, not all plaques could be identically coregistered. This may be due to nonisotropic size changes occurring during fixation of the brain for immunohistochemistry, along with minor differences in the orientation of immunohistological sectioning of the ex vivo brain compared to the MR sections of the in vivo brain, and/or differences in the thickness of the MR slice (200 μm) compared to the histological slice (40 μm).

Although the association of iron with plaques in humans and in mouse models of AD pathology is known (19,22,23,24), it remains to be established whether it is the main reason for plaque-specific T_2 contrast in MR images. As can be seen in Fig. 3, iron (III) was found to be associated with many dense-cored senile plaques, although not all Aβ plaques seen by immunohistology contained iron. Iron-loaded plaques were restricted to the cortical and hippocampal regions of the brain (Fig. 3).

We examined the utility of μMRI for detecting the development of Aβ plaques in longitudinal studies. The same mice ($N = 5$ for each group) were imaged at regular intervals of approximately one month starting at the age of 12 months. An example of MR images obtained from the brain of a Tg2576 transgenic mouse at the ages of 12, 14, 16, and 18 months is displayed in Fig. 4. A consistent increase in the MR hypointensities was observed with age in the cerebral cortical and hippocampal regions. In addition to the overall increase in MR hypointensities, the size of the circular hypointense spots also increased, suggesting an increase in the size of Aβ plaques with age (Fig. 4). Some of the Aβ plaques observed in the brain at the age of 12 months were detected consistently at all ages, while the sizes of these plaques showed an increasing trend with age (Fig. 4). Quantification of Aβ plaque load in Tg2576 mice with age is shown in Fig. 5a. A marked age-related increase in both plaque load and numerical density of the Aβ plaques is evident in this figure. Although the increase in numerical density of Aβ plaque shows an almost linear trend from 12 to 18 months of age, the overall plaque load shows a much more rapid increase from 16 to 18 months of age (Fig. 5a). An increase in the plaque load with age was associated with a significant reduction in the mean transverse relaxation time T_2 in the hippocampus and cortex of Tg2576 mice (Fig. 5b). A region in muscle, used as the internal control, did not show any significant change in T_2 relaxation time with age. The T_2 relaxation time in muscle was 27.6 ± 0.95 at the age of 12 months, and 27.9 ± 0.82 at the age of 18 months. A similar study using the age-matched nontransgenic control mice did not show any significant age-dependent decline in T_2 relaxation time in the cortex or hippocampus (Fig. 5c).

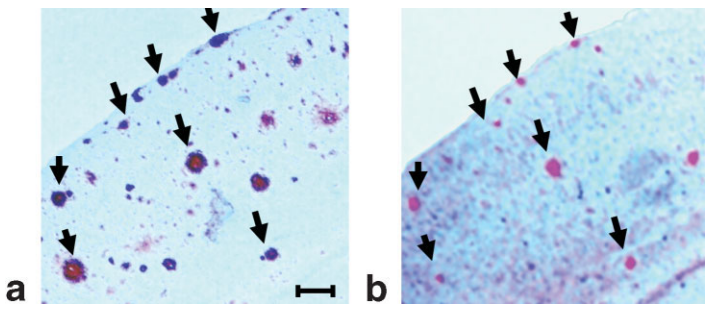

Figure 3. Coregistration of Aβ plaques and iron in adjacent brain sections of an 18-month-old Tg2576 mouse. The brain sections were stained with (**a**) an Aβ antibody (6E10) or (**b**) Perl's reaction following DAB enhancement. Arrows indicate coregistered plaques. Scale bar: 250 μm.

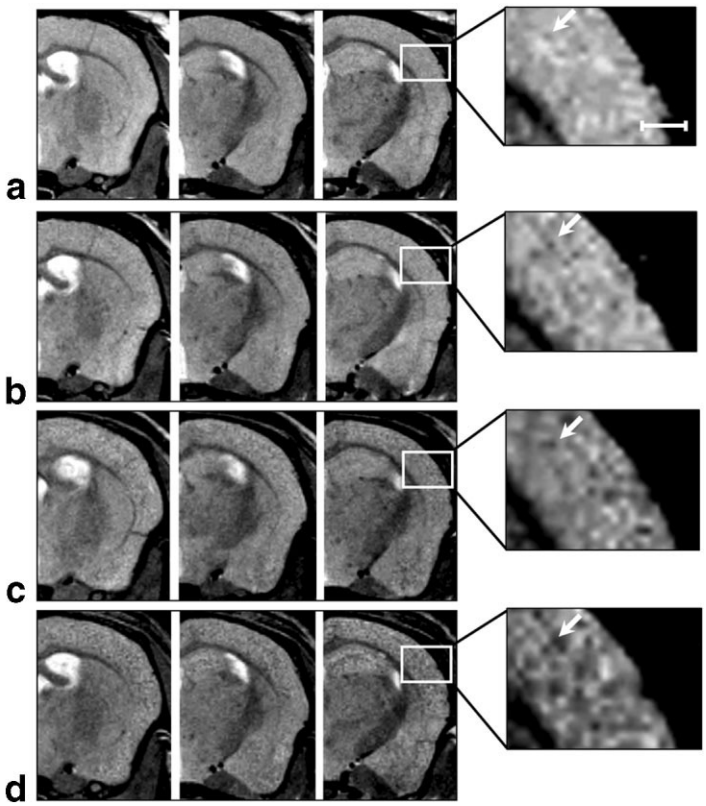

Figure 4. Development of Aβ plaques with age in the brain of AD transgenic mouse monitored by in vivo μMRI. MR images show successive coronal slices (left to right) of the brain of the same Tg2576 mouse at the ages of 12 months (**a**), 14 months (**b**), 16 months (**c**), and 18 months (**d**). Magnified subsampled areas on the right show an increase in plaque load with age. Arrows indicate the same plaque seen at 12, 14, 16, and 18 months of age. Note the increase in size with age. Scale bar: 400 μm.

DISCUSSION

This study demonstrates the application of μMRI to resolve Aβ plaque in the brain in a living transgenic mouse model of AD pathology, and to follow the development of the plaques in the same animals over time. Tg2576 mice overexpressing human APP_{695} with the "Swedish" mutation develop Aβ plaques and memory deficit with age (17,25,26,27), which makes them suitable for longitudinal MR studies.

The T_2-weighted RARE sequence used in this study allowed clear identification of hypointense lesions within a relatively short acquisition time (25 minutes), corresponding to Aβ plaques identified by immunohistochemistry (Figs. 1 and 2). In a previous study a similar fast spin-echo sequence was used to visualize plaques very clearly ex vivo in the brain of AD mice at 7T (5). Our results suggest that a similar sequence with careful adjustment of MR parameters can be applied to detect plaques in the brain in vivo at a moderately higher magnetic field of 9.4T. The typical size of Aβ plaques in Tg2576 mice varies from 20 to 150 μm. Figure 2 shows many giant plaques greater than 75 μm in diameter, which is within the spatial resolution (78 μm) of our MR experiments. Vanhoutte et al (13) recently reported in vivo visualization of Aβ plaques at 7T using intrinsic MRI contrast arising from the iron associated with plaques, using a T_2*-weighted 2D gradient-echo sequence. One of the major limitations of their study was that the plaques were seen only in the thalamus and not in the cortex or hippocampus, which are the main areas of Aβ plaque deposition in humans and all known AD transgenic mouse models. In addition,

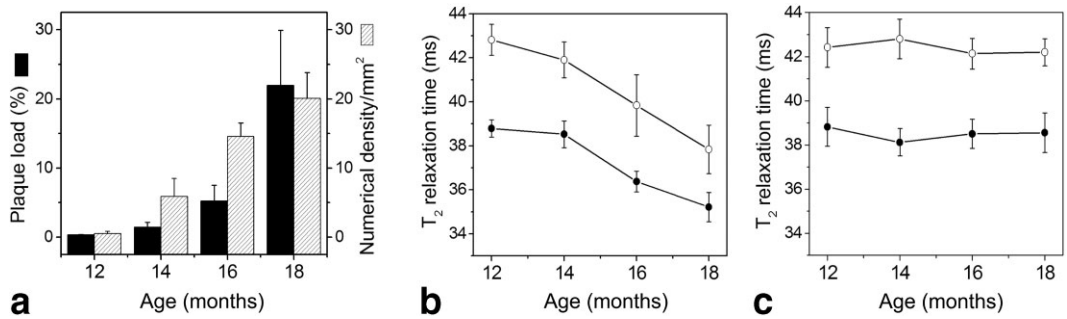

Figure 5. Age-dependent changes in Aβ plaque load and numerical density of Aβ lesions detected by μMRI (**a**) and T_2 relaxation time in the hippocampus (○) and cortex (●) regions of AD transgenic mice (**b**) and control mice (**c**). Data represent the mean of $N = 5$ (±SD).

the size of the plaques in T_2*-weighted images is often overestimated (12). Jack et al (12) recently demonstrated MRI visualization of plaques in vivo at 9.4T in another transgenic mouse model without the use of a contrast agent and using a trigger desensitizing modification of a T_2 -weighted spin-echo sequence. With this method they were able to resolve the plaques in an acquisition time as short as one hour and seven minutes. However, without trigger desensitizing modification or cardiorespiratory triggering, plaques could not be resolved (12). In the present study we used the MS RARE method employing a single excitation step followed by the collection of multiple phase-encoded echoes. With this method a good signal-to-noise ratio (SNR) was achieved with clearly identified plaques within an acquisition time of 25 minutes, with an in-plane resolution of 78μm. In addition, plaques could be resolved without any cardiorespiratory triggering or trigger desensitizing modification. It is difficult to directly compare our results with the those of Jack et al (12) due to differences in the pulse sequence and other MR parameters, as well as the different transgenic mouse models used in the studies.

The reason for plaque-specific T_2 contrast is not known. It has been speculated that the presence of iron in the Aβ plaques may be responsible for MR contrast (5,12,13,22). Defective iron homeostasis resulting in an increased iron level in AD brain has been reported (9,28). In AD brain, iron is apparently mainly concentrated in amyloid plaques and may catalyze the formation of free radicals (29). The source of this iron is unknown, but evidence suggests that induction of heme oxygenase, which occurs in AD, converts heme into tetrapyrrol and free iron (30). In AD such iron binds with the abnormal protein constituents of the lesions, e.g., Aβ. It has been shown that plaque-associated iron is redox active iron and is not bound to normal iron-binding proteins but to the abnormal protein constituents of the Aβ lesions (19,20,24). To determine whether the presence of iron is the main reason for plaque-specific T_2 contrast in MR images, we examined the distribution of iron in adjacent histological sections of the Tg2576 mouse brain. The results showed that iron is associated with many dense-cored Aβ plaques seen in the cortex as well as in the hippocampus (Fig. 3). Iron seems to be associated with the central region of the amyloid-β-deposits (Fig. 3). This observation is in line with earlier histochemical studies (19) that showed that redox active iron is specifically localized to the lesions of AD and not the glial cells surrounding senile plaques, which contain abundant iron-binding proteins. Our results suggest that iron may be the source of the intrinsic MR contrast from Aβ plaques, as was recently proposed for this mouse model (22). However, signal hypointensities arising from the reduced water content in Aβ plaques compared to the surrounding tissue and from other unknown factors cannot be ruled out.

In addition to the presence of Aβ plaques, the lateral ventricles are visible as hyperintense regions in the coronal MR slices of the brain of AD mouse at Bregma –2.4. At the same location in the brain of wild-type mice, only very small portion of lateral ventricles is seen (Fig. 1, middle row). This can be explained by the fact that AD brains show immense enlargement of the lateral ventricles due to significant loss of surrounding tissue in comparison to control brains. The ventricular enlargement in AD brains was previously shown in humans (31) and another AD mouse model (32).

As illustrated in Fig. 4, Tg2576 mice show a marked age-related increase in amyloid deposition in the hippocampal and cortical regions of the brain (Fig. 4). The plaques increase rapidly in number, size, and the degree of compactness. Only a few circular hypointense regions corresponding to Aβ plaques were observed in 12-month-old Tg2576 mice, while the density of Aβ deposits, seen as dark circular hypointense regions in the cortical and hippocampal region, considerably increased at 18 months (Fig. 4).

A quantitative estimation of Aβ plaque load and numerical density with age in the MR images shows that plaque burden increased markedly with age (Fig. 5a). The increase of plaque load was more significant after 16 months than between 12–16 months. In comparison to Aβ plaque load, the numerical density of the Aβ plaques show a linear increase between 12 and 18 months. These results can be explained by a significant increase in the size of the plaques after 16 months contributing to an increase in the plaque area in the cortex and hippocampus. These results are well in line with immunohistochemical observations (16). Since the trend toward an increase in plaque burden seen by μMRI is clearly significant at 12–18 months of age, we suggest that monitoring the effect of anti-amyloid drugs in Tg2576 mice during that time window is feasible with in vivo μMRI.

Aβ plaques in mice and humans are quite similar in size (up to 200 μm). In principle, the detection of Aβ plaques by MRI can be extended to human subjects. However, this would require improvement in instrumentation and MR sequences to permit imaging of human brain with a similar contrast-to-noise ratio (CNR) at a slightly lower spatial resolution, in a much shorter imaging time. With the growing awareness of the feasibility of human imaging at ultrahigh fields (≥7T) and improvement in RF coil technology, it may be possible to apply this approach to humans in the future (12).

The spin-spin relaxation time T_2 is a specific attribute of spins that depends on their surroundings. Interaction between spins (e.g., coupling of neighboring nuclei) destroys the phase coherence, and therefore the T_2 relaxation time can be a sensitive indicator of impaired cell physiology. A lower T_2 relaxation time was previously observed in the cortex and hippocampus of Tg2576 transgenic mice compared to nontransgenic controls (7). We followed the changes in T_2 relaxation time with age in Tg2576 transgenic mice. A good correlation was observed between the increase in the plaque load and the decrease in mean transverse relaxation time T_2 with age in both the hippocampus and cortex of Tg2576 mice (Fig. 5a and b). A similar study with age-matched nontransgenic control mice did not show any significant age-dependent decline in T_2 relaxation time (Fig. 5c). These observations suggest an influence of plaque load on T_2 reduction. Although the reason for the reduction in T_2 time is not yet clear, earlier studies

speculated that iron-associated plaques may be involved in reducing the T_2 time in AD brain (7,22).

In conclusion, we applied μMRI to resolve Aβ plaques in the brains of living transgenic AD mice without the aid of exogenous contrast agents in a reasonably short scanning time, and followed the development of the plaques in the same animals with age. Our results show that the developmental characteristics of plaque, such as number, size, and compactness, can be followed with age in the same animals using in vivo μMRI. Such longitudinal MR studies may be a valuable tool for evaluating the efficiency of novel anti-amyloid treatment strategies for arresting the growth or preventing the development of new plaques using AD mouse models.

ACKNOWLEDGMENTS

The authors thank Ingrid Hegeman for assistance in immunohistology, and Fons Lefeber and Bianca Hogers for their help with the initial μMRI measurements. We are grateful to Dr. Karen Hsiao Ashe (University of Minnesota, USA) for providing the initial three Tg2576 F1 mice for further breeding. We also thank Marion Maat-Schieman and Mark van Buchem for useful discussions.

REFERENCES

1. Frank RA, Galasko D, Hampel H, et al. Biological markers for therapeutic trials in Alzheimer's disease. Proceedings of the biological markers working group; NIA initiative on neuroimaging in Alzheimer's disease. Neurobiol Aging 2003;24:521–536.
2. Higuchi M, Iwata N, Matsuba Y, Sato K, Sasamoto K, Saido TC. ^{19}F and ^{1}H MRI detection of amyloid-β plaques in vivo. Nat Neurosci 2005;8:527–533.
3. Golde TE. Alzheimer disease therapy: can the amyloid cascade be halted? J Clin Invest 2003;111:11–18
4. Wengenack TM, Curran GL, Poduslo JF. Targeting Alzheimer amyloid plaques in vivo. Nat Biotechnol 2000;18:868–872.
5. Lee SP, Falangola MF, Nixon RA, Duff K, Helpern JA. Visualization of β-amyloid plaques in a transgenic mouse model of Alzheimer's disease using MR microscopy without contrast agents. Magn Reson Med 2004;52:538–544.
6. Benveniste H, Einstein G, Kim KR, Hulette C, Johnson GA. Detection of neuritic plaques in Alzheimer's disease by magnetic resonance microscopy. Proc Natl Acad Sci USA 1999;96:14079–14084.
7. Helpern JA, Lee SP, Falangola MF, et al. MRI assessment of neuropathology in a transgenic mouse model of Alzheimer's disease. Magn Reson Med 2004;51:794–798.
8. Zhang J, Yarowsky P, Gordon MN, et al. Detection of amyloid plaques in mouse models of Alzheimer's disease by magnetic resonance imaging. Magn Reson Med 2004;51:452–457.
9. Poduslo JF, Wengenack TM, Curran GL, et al. Molecular targeting of Alzheimer's amyloid plaques for contrast-enhanced magnetic resonance imaging. Neurobiol Dis 2002;11:315–329.
10. Wadghiri YZ, Singurdsson EM, Sadowski M, et al. Detection of Alzheimer's Amyloid in transgenic mice using magnetic resonance microimaging. Magn Reson Med 2003;50:293–302.
11. Skovronsky DM, Zhang B, Kung MP, Kung HF, Trojanowski JQ, Lee VMY. *In vivo* detection of amyloid plaques in a mouse model of Alzheimer's disease. Proc Natl Acad Sci USA 2000;97:7609–7614.
12. Jack CR, Garwood M, Wengenack TM, et al. In vivo visualization of Alzheimer's amyloid plaques by magnetic resonance imaging in transgenic mice without a contrast agent. Magn Reson Med 2004; 52:1263–1271.
13. Vanhoutte G, Dewachter I, Borghgraef P, van Leuven F, Van der Linden A. Noninvasive in vivo MRI detection of neuritic plaques associated with iron in APP[V717I] transgenic mice, a model for Alzheimer's disease. Magn Reson Med 2005;53:607–613.
14. Apelt J, Kumar A, Schliebs R. Impairment of cholinergic neurotransmission in adult and aged transgenic Tg2576 mouse brain expressing the Swedish mutation of human β-amyloid precursor protein. Brain Res 2002;953:17–30.
15. Apelt J, Schliebs R. β-Amyloid-induced glial expression of both pro-and anti-inflammatory cytokines in cerebral cortex of aged transgenic Tg2576 mice with Alzheimer plaque pathology. Brain Res 2001;894:21–30.
16. Sasaki A, Shoji M, Harigaya Y, et al. Amyloid cored plaques in Tg2576 transgenic mice are characterized by giant plaques, slightly activated microglia, and the lack of paired helical filament typed, dystrophic neurites. Virchows Arch 2002;441:358–367.
17. Hsiao K, Chapman P, Nilsen S, et al. Correlative memory deficits, Aβ elevation, and amyloid plaques in transgenic mice. Science 1996;274:99–103.
18. Henning J, Nauerth A, Friedburg H. RARE imaging: a fast imaging method for clinical MR. Magn Reson Med 1986;3:823–833.
19. Smith MA, Harris PLR, Sayre LM, Perry G. Iron accumulation in Alzheimer disease is a source of redox-generated free radicals. Proc Natl Acad Sci USA 1997;94:9866–9868.
20. Smith MA, Hirai K, Hsiao K, et al. Amyloid-beta deposition in Alzheimer transgenic mice is associated with oxidative stress. J Neurochem 1998;70:2212–2215.
21. van Balen R, Koelma D, Ten Kate TK, Mosterd B, Smeulders AWM. SCIL Image: a multi-layered environment for use and development of image processing software. In: Christensen RW, Crowley JL, editors. Experimental environments for computer vision and image processing. Singapore: World Scientific Publishing Co. Ltd., 1994. p 107–126.
22. Falangola MF, Lee SP, Nixon RA, Duff K, Helpern JA. Histological co-localization of iron in Aβ Plaques of PS/APP transgenic mice. Neurochem Res 2005;30:201–205.
23. Atwood CS, Martins RN, Smith MA, Perry G. Senile plaque composition and posttranslational modification of amyloid-beta peptide and associated proteins. Peptides 2002;23:1343–1350.
24. Bush AI, Pettingell WH, Multhaup G, et al. Rapid induction of Alzheimer Aβ amyloid formation by zinc. Science 1994;265:1464–1467.
25. Westerman MA, Cooper-Blacketer D, Mariash A, et al. The relationship between Abeta and memory in the Tg2576 mouse model of Alzheimer's disease. J Neurosci 2002;22:1858–1867.
26. Klinger M, Apelt J, Kumar A, et al. Alterations in cholinergic and non-cholinergic neurotransmitter receptor densities in transgenic Tg2576 mouse brain with β-amyloid plaque pathology. Int J Dev Neurosci 2003;21:357–369.
27. Apelt J, Bigl M, Wunderlich P, Schliebs R. Aging-related increase in oxidative stress correlates with developmental pattern of beta-secretase activity and beta-amyloid plaque formation in transgenic Tg2576 mice with Alzheimer-like pathology. Int J Dev Neurosci 2004;22:475–484.
28. Gelman BB. Iron in CNS disease. J Neuropathol Exp Neurol 1995; 54:477–486.
29. Markesbery WR, Carney JM. Oxidative alterations in Alzheimer's disease. Brain Pathol 1999;9:133–146.
30. Salinas M, Diaz R, Abraham NG, Ruiz de Galarreta CM, Cuadrado A. Nerve growth factor protects against 6-hydroxydopamine-induced oxidative stress by increasing expression of heme oxygenase-1 in a phosphatidylinositol 3-kinase-dependent manner. J Biol Chem 2003;278:13898–13904.
31. Schott JM, Price SL, Frost C, Whitwell JL, Rossor MN, Fox NC. Measuring atrophy in Alzheimer disease: a serial MRI study over 6 and 12 months. Neurology 2005;65:119–124.
32. Feng R, Wang H, Wang J, Shrom D, Zeng X, Tsien JZ. Forebrain degeneration and ventricle enlargement caused by double knockout of Alzheimer's *presenilin-1* and *presenilin-2*. Proc Natl Acad Sci USA 2004;101:8162–8167.